Calibrating the coevolution of Ediacaran life and environment

Alan D. Rooney[a,1], Marjorie D. Cantine[b,1], Kristin D. Bergmann[b], Irene Gómez-Pérez[c], Badar Al Baloushi[c], Thomas H. Boag[d], James F. Busch[e], Erik A. Sperling[d], and Justin V. Strauss[e]

[a]Department of Earth and Planetary Sciences, Yale University, New Haven, CT 06520; [b]Department of Earth, Atmospheric, and Planetary Sciences, Massachusetts Institute of Technology, Cambridge, MA 02139; [c]Petroleum Development Oman, Exploration Directorate, Muscat 100, Oman; [d]Department of Geological Sciences, Stanford University, Stanford, CA 94305; and [e]Department of Earth Sciences, Dartmouth College, Hanover, NH 03755

Edited by Paul F. Hoffman, University of Victoria, Victoria, BC, Canada, and approved June 1, 2020 (received for review February 15, 2020)

The rise of animals occurred during an interval of Earth history that witnessed dynamic marine redox conditions, potentially rapid plate motions, and uniquely large perturbations to global biogeochemical cycles. The largest of these perturbations, the Shuram carbon isotope excursion, has been invoked as a driving mechanism for Ediacaran environmental change, possibly linked with evolutionary innovation or extinction. However, there are a number of controversies surrounding the Shuram, including its timing, duration, and role in the concomitant biological and biogeochemical upheavals. Here we present radioisotopic dates bracketing the Shuram on two separate paleocontinents; our results are consistent with a global and synchronous event between 574.0 ± 4.7 and 567.3 ± 3.0 Ma. These dates support the interpretation that the Shuram is a primary and synchronous event postdating the Gaskiers glaciation. In addition, our Re-Os ages suggest that the appearance of Ediacaran macrofossils in northwestern Canada is identical, within uncertainty, to similar macrofossils from the Conception Group of Newfoundland, highlighting the coeval appearance of macroscopic metazoans across two paleocontinents. Our temporal framework for the terminal Proterozoic is a critical step for testing hypotheses related to extreme carbon isotope excursions and their role in the evolution of complex life.

Neoproterozoic | Shuram | Re-Os geochronology | Ediacaran | carbon isotopes

In addition to recording the radiation of animals (1), extreme climate events (2), oscillating global redox conditions (3–5), and geomagnetic instability that could be linked to rapid plate motion (6, 7), Neoproterozoic rocks host Earth's most negative carbon isotope excursions (CIEs) (8). These CIEs have been interpreted to record perturbations to the global carbon cycle of a magnitude unlike any recorded before or since (9). The largest among them, the Shuram CIE is globally represented by an abrupt ∼17‰ drop from enriched carbonate carbon isotope ($\delta^{13}C_{carb}$) values to highly depleted values of −12‰, before slowly recovering to a less enriched background state (10) (Fig. 1). Despite being recorded across more than six paleocontinents and a variety of depositional settings, the Shuram CIE has remained one of the most enigmatic geochemical events of the Proterozoic Eon, with three key controversies surrounding this event: 1) its onset and duration (11, 12); 2) its primary or diagenetic origin (13–15); and 3) its temporal proximity and causal relationship to marine redox fluctuations, glaciation, and the evolution and/or extinction of the Ediacaran biota (16–20).

Statistical analyses indicate that Ediacaran macrofossils can be assigned into three distinct recurrent taxonomic associations, termed assemblages, that may reflect successive episodes of biotic turnover (23, 24). The rise and fall of Ediacaran assemblages is not well constrained geochronologically, and the apparent appearances and disappearances of these assemblages may also be subject to potential paleoenvironmental biases. The earliest Avalon assemblage, which consists almost exclusively of fossils preserved in marine slope and basinal depositional environments, is dominated by large fractal organisms (termed fronds) and possible sponges and cnidarians (25). The younger, more diverse White Sea assemblage includes more complex and mobile taxa such as *Dickinsonia* and the bilaterian *Kimberella* and largely occurs in marine subtidal to intertidal shelf settings (26). Finally, the terminal Ediacaran Nama assemblage is highly depauperate and dominated by early bilaterian trace fossils, tubiculous fauna, and the earliest biomineralizing animals, all of which occur in a variety of shallow-marine carbonate and siliciclastic environments (27). Although these assemblages appear to hold up across Ediacaran paleocontinents, the fundamental lack of Ediacaran geochronological constraints has precluded linking biotic turnover to key tectonic or biogeochemical perturbations, such as the Shuram CIE (28, 29).

In the absence of a reliable chronology, two age models for the Shuram CIE and its relationship to Ediacaran geoevents and bioevents have emerged (28). Both presume the termination occurs circa 550 Ma, an assumption informed by an ash dated to 551.1 ± 0.7 Ma above the Shuram CIE in the Doushantuo Formation of South China (30), and which puts the CIE in association with a purported extinction of the White Sea assemblage (18, 19). Critically, however, these models differ in placing the onset of the Shuram CIE at circa 580 Ma (thus potentially linked with the Gaskiers glaciation; ref. 17) versus circa 560 Ma. As a result, estimates for the duration of the excursion range from <10 to ∼30 My, highlighting an ambiguity in current Ediacaran chronologies that makes it impossible to confidently link the Shuram CIE to global biogeochemical cycles or the radiation or extinction of soft-bodied Ediacaran fossils.

Significance

Our understanding of the interactions between animal evolution, biogeochemical cycling, and global tectonics during the Ediacaran Period (635 to 541 Ma) is severely hampered by lack of a robust temporal framework. The appearance and extinction of the earliest fossil animals are hypothesized to correlate with upheavals in biogeochemical cycles—foremost the Shuram carbon isotope excursion, possibly the largest known disturbance to the global carbon cycle. However, without age constraints on the excursion's timing and duration, its driving mechanisms, global synchroneity, and role in Ediacaran geobiological evolution cannot be evaluated. We provide radioisotopic ages for the onset and termination of the Shuram, evaluate its global synchroneity, and show that it is divorced from the rise of the earliest preserved animal ecosystems.

Author contributions: A.D.R., K.D.B., and J.V.S. designed research; A.D.R., M.D.C., I.G.-P., B.A.B., T.H.B., J.F.B., E.A.S., and J.V.S. performed research; I.G.-P. contributed new reagents/analytic tools; A.D.R., M.D.C., I.G.-P., B.A.B., J.F.B., and J.V.S. analyzed data; and A.D.R., M.D.C., and K.D.B. wrote the paper with contributions from all authors.

The authors declare no competing interest.

This article is a PNAS Direct Submission.

[1]To whom correspondence may be addressed. Email: alan.rooney@yale.edu or mcantine@mit.edu.

This article contains supporting information online at https://www.pnas.org/lookup/suppl/doi:10.1073/pnas.2002918117/-/DCSupplemental.

First published July 6, 2020.

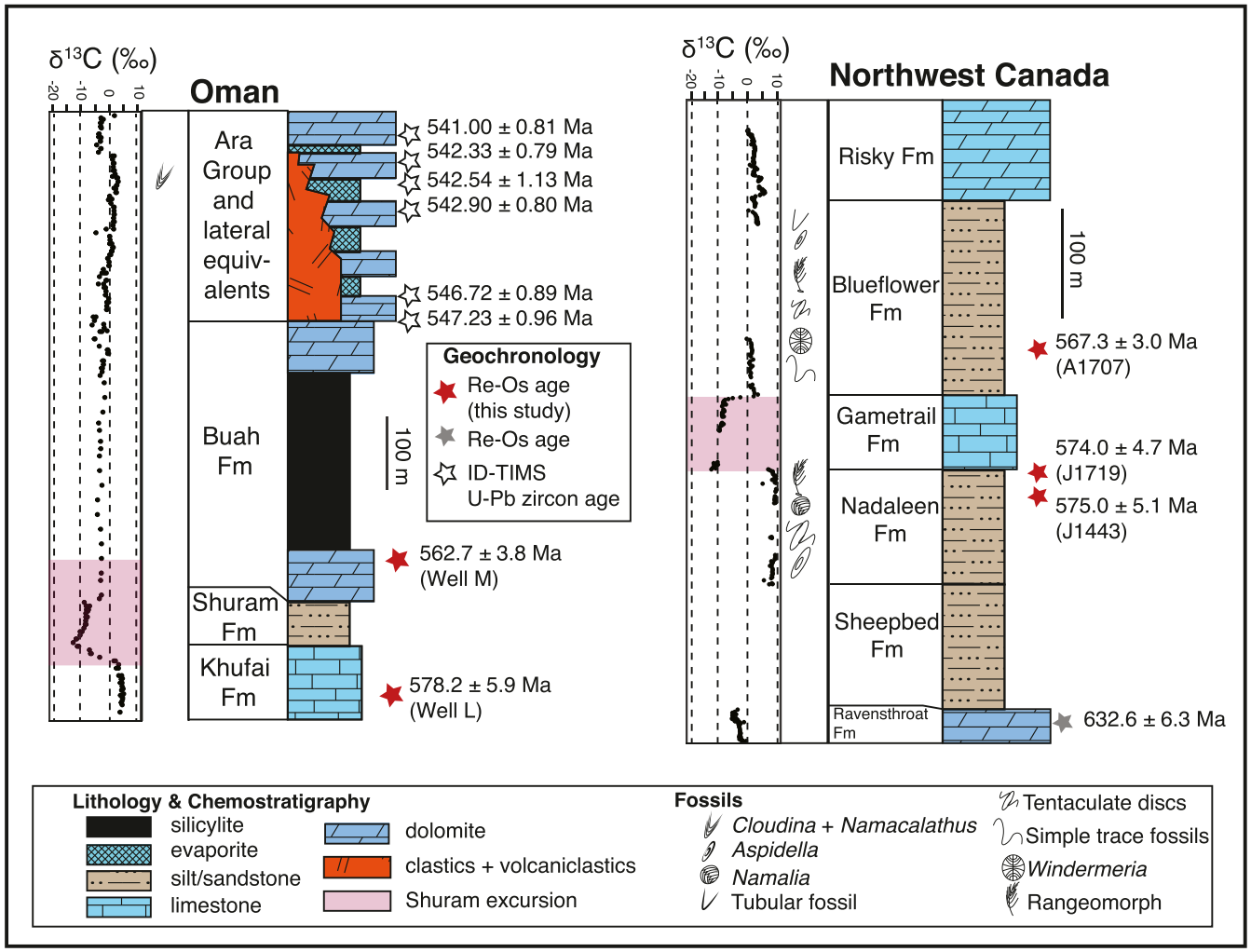

Fig. 1. Simplified stratigraphy and chemostratigraphy of Ediacaran sedimentary rocks in northwestern Canada and Oman. Sampled horizons indicated with stars and compilation of carbon isotope data are in *SI Appendix*, Table S1. Previously published geochronological constraints are from U-Pb zircon ages on ash beds (21) and Re-Os ages on organic-rich sedimentary rocks (22). Fm, Formation.

Developing a high-resolution chronology for the Shuram CIE has proven difficult as Ediacaran fossil assemblages only have broad assemblage-scale biostratigraphic utility and previous radioisotopically dated horizons only have provided loose constraints on the Shuram CIE's termination (21, 30). Moreover, chemostratigraphic correlations of well-dated fossiliferous Ediacaran successions, such as the Conception Group of Newfoundland (17) or the Charnian Supergroup of the United Kingdom (31), are not possible due to the paucity of carbonate sedimentation in those basins. Here, we present a high-resolution chronology for the Shuram CIE with five rhenium-osmium (Re-Os) dates from mixed carbonate and siliciclastic sedimentary rocks bracketing the excursion on two different paleocontinents (Figs. 1 and 2). To develop this age model, we collected organic-rich shale and calcareous mudstone samples from the Ediacaran Nafun Group of Oman and the Rackla Group of Yukon, Canada, respectively (Fig. 1 and *SI Appendix*, Figs. S1 and S2). These dates provide critical insights into the timing and tempo of biological innovations and environmental upheavals during the terminal Proterozoic.

Geological Setting of the Nafun (Oman) and Rackla (Canada) Groups

The Ediacaran Nafun Group of Oman is exposed in the central Huqf Desert and northern Oman in the Al Hajar Mountains, and penetrated by multiple drill cores in the South Oman Salt Basin and Huqf–Haushi High areas (*SI Appendix*, Fig. S1). In the subsurface and in outcrops of the Huqf Desert, the Nafun Group has not undergone significant metamorphism or deformation, and its sedimentology, stratigraphy, and geochemistry has been extensively studied (32–39). Radioisotopic constraints on the Nafun Group are limited to minimum depositional ages derived from detrital zircons (21, 40), although extensive dating of volcaniclastic and ash units in the overlying Ara Group and Fara Formation have yielded latest Ediacaran ages (21).

The Khufai Formation of the Nafun Group is predominantly carbonate and lies stratigraphically above a Cryogenian (circa 635 Ma) Marinoan diamictite and cap carbonate succession. The onset of the Shuram CIE is captured in the uppermost Khufai Formation (32). The transition to the overlying eponymous Shuram Formation is marked by a sharp shift to siltstone with occasional interbedded limestone, which increases in abundance moving up-section (32, 37, 38). These interbedded limestone strata record the nadir of the Shuram CIE and its subsequent shift to less negative $\delta^{13}C_{carb}$ values; full recovery occurs in the overlying carbonate-rich Buah Formation (*SI Appendix*, Fig. S2 and Table S1). In deep-water sections, like those sampled for this study, a thick silicyte (rock containing >90% cryptocrystalline silica) occurs in the upper Buah Formation (41). An unconformity between the Buah Formation and overlying carbonate and evaporite of the Ara Group is often seen in the subsurface; in the

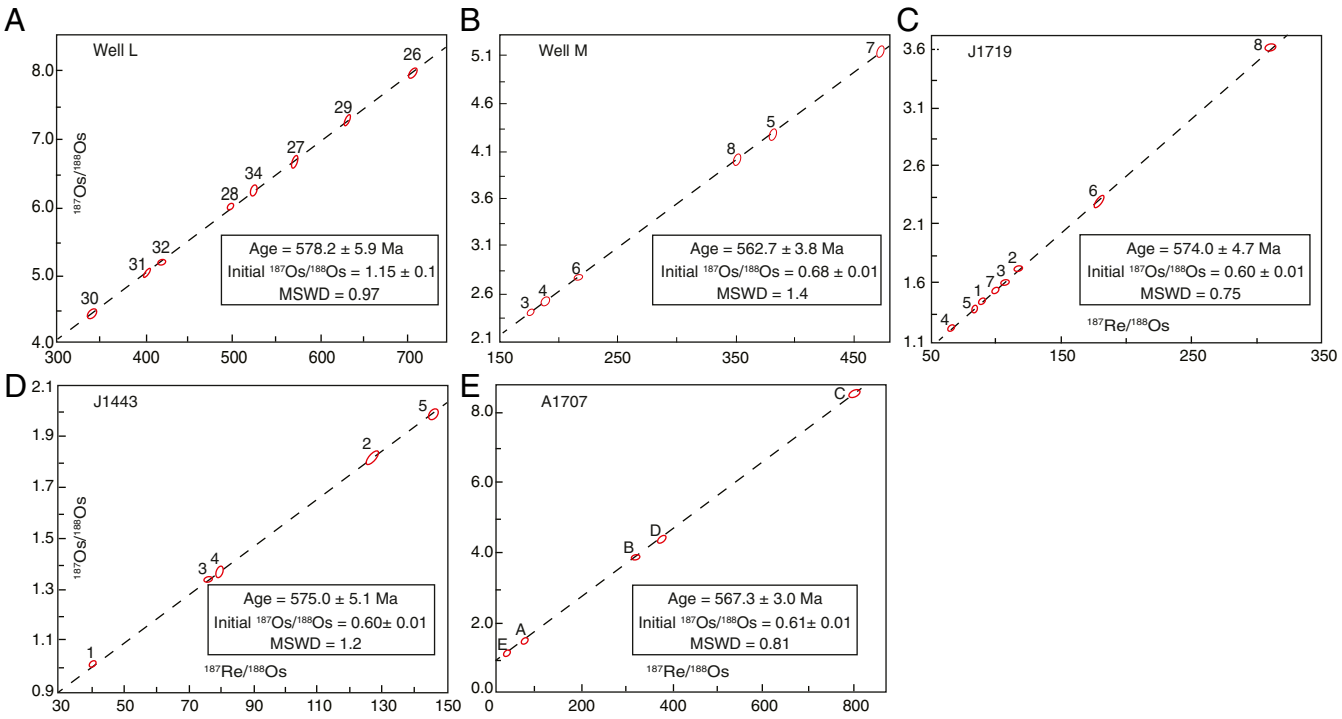

Fig. 2. Re-Os isochron diagrams for dated horizons. (*A*) Well L: Khufai Formation, Oman. (*B*) Well M: Buah Formation, Oman. (*C*) J1719: Nadaleen Formation, Wernecke Mountains, Yukon. (*D*) J1443: Nadaleen Formation, Wernecke Mountains, Yukon. (*E*) A1707: unit PH4, Ogilvie Mountains, Yukon. All isotopic composition and elemental abundance data are presented in *SI Appendix*, Table S2.

Oman Mountains, the Buah is overlain by volcaniclastic strata of the Fara Formation (39, 42, 43). Fossils of Ediacaran biota are not known from any Nafun Group strata, but *Cloudina* and *Namacalathus* are reported in Ara Group drill core (44). Two cores, Well L and Well M, drilled by Petroleum Development Oman in the last decade, sample the deepest water environments of the South Oman Salt Basin (*SI Appendix*, Fig. S1). The stratigraphic position of samples from Wells L and M are shown within the context of Thamoud-6, a deep-water well that has been described previously (10, 34, 37, 39, 44) (*SI Appendix*, Figs. S1 and S2).

The Rackla Group is exposed throughout the Mackenzie, Wernecke, and Ogilvie Mountains of Yukon and Northwest Territories, Canada (45) (Fig. 1 and *SI Appendix*, Fig. S3). Rackla Group strata in the Wernecke and Mackenzie Mountains overlie a circa 635 Ma Marinoan glacial-cap carbonate succession and begin with the Sheepbed Formation, the base of which is dated to 632.1 ± 5.9 Ma (22). The Sheepbed Formation is overlain by mixed carbonate and siliciclastic strata of the Nadaleen Formation (45) (previously termed "June beds" in ref. 29), which hosts Avalon assemblage Ediacaran macrofossils, including the discoid fossils *Aspidella* and *Hiemolora*, the erniettomorph *Namalia*, and various rangeomorphs (46). The Nadaleen has highly enriched $\delta^{13}C_{carb}$ values up to +9‰ (Fig. 1). The overlying carbonate-dominated Gametrail Formation hosts an abrupt drop in $\delta^{13}C_{carb}$ values as low as −13‰ within the nadir of the Shuram CIE (29, 45), before recovering to values around 0 to +2 near the contact with the overlying Blueflower Formation. The Blueflower contains a diverse assemblage of trace fossils, rangeomorphs, tubular and discoid fossils, and a putative dickinsoniid (47). These strata are followed by the terminal Ediacaran carbonate-dominated Algae and Risky formations, which are both unconformably overlain by lowermost Cambrian strata of the Narchilla and Ingta formations, respectively, which host small shelly and diverse trace fossil assemblages (29, 45).

Ediacaran strata of the Ogilvie Mountains (Rackla Group) comprise a series of informal map units labeled PH3 and PH4 (29, 48, 49) (*SI Appendix*, Fig. S3). Unit PH3 consists predominantly of black shale that directly overlies an unnamed Cryogenian glacial deposit and cap carbonate pair belonging to the circa 635-Ma Marinoan glaciation (29). This is succeeded by the Shuram CIE-bearing unit PH4, which records an abrupt shift to highly depleted $\delta^{13}C_{carb}$ values down to −9‰ (45) (*SI Appendix*, Table S1). A concretionary limestone unit at the top of unit PH4 has been loosely correlated with the Blueflower Formation and records a return to enriched $\delta^{13}C_{carb}$ values of 0 to +2‰ (*SI Appendix*, Fig. S3). Units PH3 and PH4 are truncated by an angular unconformity beneath informal unit PH5, which is composed of siltstone and sandstone that contain diagnostic early–middle Cambrian trace fossils (48).

Re-Os Geochronology

Two samples of organic-rich shale of the Khufai and Buah formations were retrieved from Well L and Well M of the South Oman Salt Basin for Re-Os geochronology (Fig. 1; *SI Appendix*, Fig. S1; and *Materials and Methods*). Samples from Well L of the basal Khufai Formation were deposited prior to the onset of the Shuram CIE and yield a Re-Os depositional age of 578.2 ± 5.9 Ma (2σ, $n = 7$, mean square of weighted deviates [MSWD] = 0.97 [all isochrons generated in this study are model 1, and total uncertainties include the uncertainty in the ^{187}Re constant, λ; ref. 50]), with an initial $^{187}Os/^{188}Os$ (Osi) value of 1.15 ± 0.05 (Fig. 2*A* and *SI Appendix*, Table S2). Buah Formation samples from Well M, which record the post-Shuram recovery to positive $\delta^{13}C_{carb}$ values, yield a depositional age of 562.7 ± 3.8 Ma (2σ, $n = 7$, MSWD = 1.40) with an Osi value of 0.68 ± 0.01 (Fig. 2*B*).

Three samples from black calcareous mudstone horizons in the Rackla Group were sampled for Re-Os geochronology in order to bracket the Shuram CIE in northwestern Canada (Figs. 1 and 2 and *SI Appendix*). Sample J1719 of the upper Nadaleen Formation in the Wernecke Mountains yields a pre-Shuram Re-Os depositional age of 574.0 ± 4.7 Ma (2σ, $n = 8$, MSWD = 0.75) with an Osi value of 0.60 ± 0.01 (Fig. 2*C*), and sample J1443 of the upper Nadaleen Formation yields a similar depositional age of 575.0 ± 5.1 Ma (2σ, $n = 5$, MSWD = 1.20) with an Osi value of 0.60 ± 0.01 (Fig. 2*D*). Above the Shuram CIE, sample A1707 from map unit PH4 in the Ogilvie Mountains yields a post-Shuram depositional age of

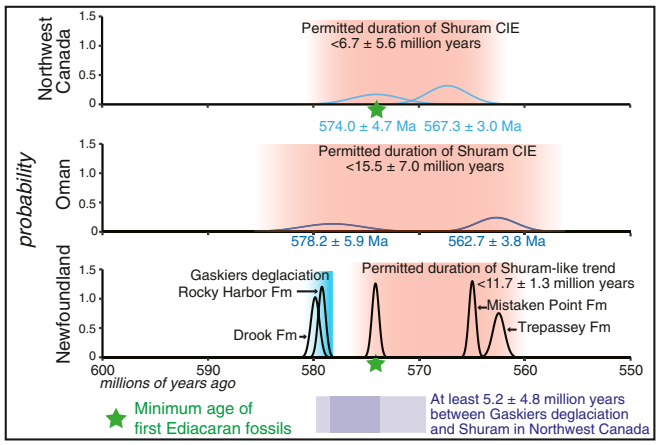

Fig. 3. Probability distributions of ages from this study and others (17, 51, 52) (note use of age from ref. 52 for the Pizza Disc ash bed used both as 1) the minimum age of the first Ediacara biota preserved in Newfoundland and 2) the maximum age of the Shuram-like isotope trend described by ref. 51). The minimum duration of the Shuram CIE or Shuram-like isotope trend in each location is shown. Assuming a synchronous global Shuram CIE, the preonset age (574.0 ± 4.7 Ma) from northwestern Canada suggests at least 5.2 ± 4.8 My between Gaskiers deglaciation and the onset of the CIE. This is supported by a recently observed isotope trend in siliciclastic-hosted carbonate in Newfoundland (51), which may be correlative to the Shuram CIE and is stratigraphically and geochronologically distinct from the Gaskiers deglaciation. An ash in the Trepassey Formation (Fm) above this trend constrains it to >562.5 ± 1.1 Ma (51); an ash within the Mistaken Point Fm, associated with negative values, is dated to 565.00 ± 0.64 Ma (52). Ages in blue are Re-Os ages from organic-rich rocks (this study); all others are chemical abrasion–isotope dilution–thermal ionization mass spectrometry U-Pb ages measured on zircon (17, 51, 52).

567.3 ± 3.0 Ma (2σ, n = 6, MSWD = 0.81) with an Osi value of 0.61 ± 0.04 (Fig. 2*E*).

Onset, Duration, and Synchroneity of the Shuram CIE Excursion

The geochronological data presented here yield consistent and overlapping age constraints for the onset and termination of the Shuram CIE on separate paleocontinents. In Oman, onset of the excursion occurred after 578.2 ± 5.9 Ma, with termination by 562.7 ± 3.8 Ma; the excursion's duration in Oman is thus constrained to be less than 15.5 ± 7.0 My (Fig. 3). In northwestern Canada, the excursion is constrained to have lasted no more than 6.7 ± 5.6 My, beginning after 574.0 ± 4.7 Ma and ending by 567.3 ± 3.0 Ma (Fig. 3 and *SI Appendix*, Tables S1 and S3). A recent study of siliciclastic-hosted $\delta^{13}C_{carb}$ data from fossiliferous strata in the Conception Group of Newfoundland noted an isotopic trend, potentially correlative with the Shuram CIE (51), that is temporally constrained between 574.17 ± 0.66 and 562.5 ± 1.1 Ma (17, 51, 52). These dates are compatible with those from Oman and northwestern Canada, and if this isotopic trend is correlative with the Shuram CIE, these data suggest a duration in Newfoundland of less than 11.7 ± 1.3 My (Fig. 3). Critically, the Re-Os dates from northwestern Canada and Oman demonstrate that the Shuram CIE is recorded in coeval strata on multiple paleocontinents within analytical uncertainty, consistent with a global and synchronous event. These constraints also permit interpretation of the Shuram CIE as a series of short and asynchronous events in separate basins in this time window. However, the Shuram CIE—which exhibits remarkable consistency in its expression across multiple successions (9)—is more parsimoniously interpreted as a single isochronous event. The congruence of ages from multiple paleocontinents also suggests an accuracy for the mean ages that is greater than the strict uncertainty derived for individual ages. Interpretation of the Shuram CIE as a synchronous event indicates that the excursion occurred in all locations after 574.0 ± 4.7 Ma. This temporal framework indicates the Shuram CIE is at least 5.2 ± 4.8 My younger than the Gaskiers deglaciation (17), severing a potential mechanistic link to the immediate aftermath of glaciation as a driver for the excursion (Fig. 3).

Toward Calibration of the Ediacaran Period

The dates presented herein have important implications for the appearance of macroscopic eukaryotes in the fossil record of northwestern Canada and globally (Fig. 4). A recently dated ash in the Drook Formation of Newfoundland ∼25 m above the first appearance of ivesheadiomorphs and frondose fossils constrains the appearance of the Ediacaran biota to >574.17 ± 0.66 Ma (52) (Fig. 4). The 574.0 ± 4.7 Ma Re-Os date from the Nadaleen Formation is identical, within uncertainty, suggesting these organisms were globally distributed and likely appeared before the Shuram CIE based on their stratigraphic distribution in northwestern Canada (Fig. 4). It has been proposed that Avalon taxa originally evolved in deep-water habitats as a physiological refuge (53); the significance of this synchronous first appearance datum in northwestern Canada and Newfoundland remains unclear, but it is at least consistent with the hypothesis that deep-water slope environments on different continental margins harbored early macroscopic life.

Calibration of the Shuram CIE also unexpectedly divorces the stratigraphic and/or evolutionary appearance and disappearance of the Ediacara biota from previously hypothesized environmental drivers (16, 18). Based on the available data, the Avalon assemblage appears after the Gaskiers glaciation but before the onset of the Shuram CIE and associated marine oxygenation (Figs. 3 and 4 and *SI Appendix*). The geochronological data reported herein support a revised age model for Member IV of the Doushantuo Formation of South China, now assigning Member IV (which records the termination of the Shuram CIE) an age of circa 565 Ma (30). This means that modeled estimates of the areal extent of global seafloor euxinia derived from δ^{98}Mo data in Doushantuo Member IV euxinic shale and δ^{238}U data from uppermost Doushantuo Member III carbonates (54) are older than previously assumed, with proposed global ocean oxygenation occurring by circa 565 instead of 550 Ma (16, 54). This is in strong contrast with the pre-Shuram interval, when 25 to 100% of the global seafloor was estimated to be anoxic (Fig. 4), thereby implying an ocean oxygenation event is associated with the Shuram CIE. It was hypothesized that this oxygenation may have driven or otherwise allowed for the appearance of the White Sea assemblage (16) due to their likely higher oxygen requirements (55); however, our age model for the Ediacaran Period indicates that marine oxygenation as recorded in these geochemical proxies significantly predates the appearance of White Sea assemblage fossils. There actually may be little to no published redox geochemical data that is demonstrably from the circa 560 to 555 Ma window when the White Sea assemblage first appears in the fossil record. In contrast to recent suggestions (18, 19), the temporal constraints on the Shuram CIE presented here suggest it is disconnected from the extinction of the White Sea assemblage at circa 550 Ma (Fig. 4).

There are still important nuances to consider in connecting the Shuram CIE with records of animal evolution, including preservational controls on the appearance of fossils (56) and long-enduring questions of the permissible temporal lag between environmental change and biotic response. However, our temporal framework for the terminal Proterozoic suggests that evolutionary dynamics in the Ediacaran Period were, at face value, potentially decoupled from dramatic environmental changes. This finding highlights the importance of a robust geochronological framework for linking Proterozoic environmental change with the fossil record.

The synchronous onset and termination of the Shuram CIE in at least two, but possibly three, sedimentary successions from different paleocontinents with different lithological expressions and sediment accumulation rates is difficult to reconcile with a diagenetic origin for the excursion. Alteration by hydrothermal (13) or meteoric waters (15) would not be expected to produce similar styles of alteration of different lithofacies over variable stratigraphic thicknesses of similar durations. Moreover, the Shuram CIE is virtually unique in its stratigraphic expression and well characterized in marine strata over multiple paleocontinents and paleolatitudes (9); our documentation herein of its occurrence within radioisotopic analytical uncertainty across different paleocontinents bolsters interpretation

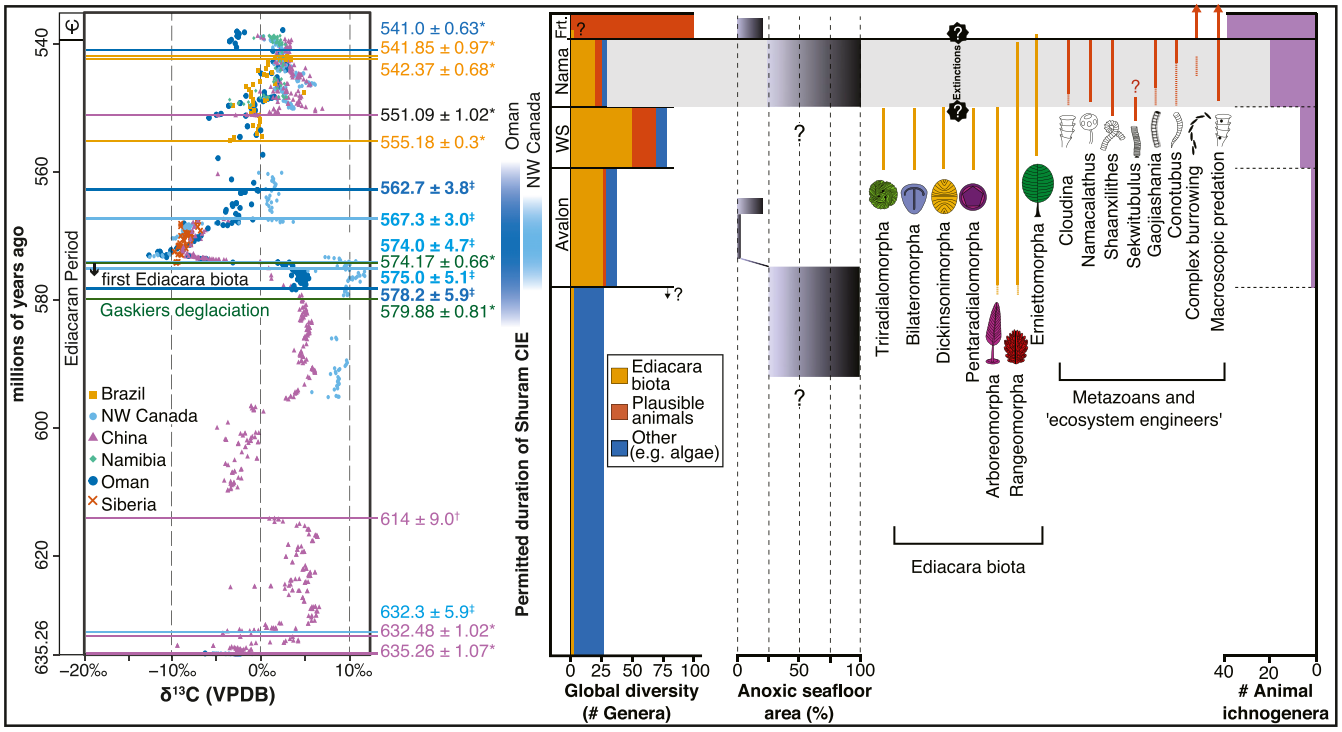

Fig. 4. Composite carbon isotope curve, age constraints, and fossil occurrences for the Ediacaran Period. References used for carbon isotope curve and age model are listed in the *SI Appendix*. *, U-Pb TIMS zircon date; †, U-Pb SHRIMP zircon date; ‡ indicates Re-Os date. The same color is used to plot both ages and chemostratigraphic data from the same location; dark green ages are from Newfoundland. Dates in bold are Re-Os ages from this study; bolded dark blue ages are from Oman, and bolded light blue ages are from northwestern Canada. Global diversity, ranges of Ediacara biota constituents, and animal ichnogenera follow (18). Percent anoxic seafloor area derived from mass balance modeling of Mo and U isotopic data are from refs. 16, 54. WS, White Sea; Frt., Fortunian; £, Cambrian.

of the Shuram CIE as a primary global event—potentially one of the largest global carbon cycle perturbations in Earth's history. These geochronological data do not necessarily require that the Shuram CIE record global open-marine dissolved inorganic carbon (DIC) isotopic compositions; a range of carbonate platform-related processes (e.g., refs. 57–59) may result in discontinuities in the isotopic compositions of different DIC pools. Critically, these dates provide key information for assessing these and other mechanisms capable of generating such a large, synchronous, and sustained shift in the isotopic composition of Ediacaran carbonate systems.

Conclusions

Radioisotopic dates for the onset and termination of the Shuram CIE across multiple paleocontinents provide evidence for the CIE as a primary and synchronous global event lasting no more than 6.7 ± 5.6 My. Together with associated redox geochemical data from coeval sedimentary successions (16, 29, 54), these geochronological data also connect the highly depleted $\delta^{13}C_{carb}$ values of the Shuram CIE to a period of relative ocean oxygenation. This resolved chronology for the Ediacaran Period decouples the Shuram CIE from the Gaskiers glaciation circa 580 Ma and the extinction of the White Sea fauna circa 550 Ma and highlights the coeval appearance of macroscopic metazoans across two paleocontinents (Fig. 4). This emerging chronology provides essential context for evaluating the mechanisms capable of driving an extraordinarily negative and extended CIE and assessing its impact on the habitats and evolution of early animals.

Materials and Methods

Sampling for Re-Os Geochronology. Approximately 30 g of carbonaceous shale and mudstone was sampled from outcrop and drill core in the Nadaleen, Blueflower, Khufai, and Buah Formations, as well as map unit PH4. Similar to methods outlined previously (60), for outcrop samples, an approximately 25-cm-deep trench was dug into the outcrop to avoid sampling surficial weathered material, and sampling was undertaken horizontally for up to 65 cm along a single <3-cm-thick horizon to maximize the spread of $^{187}Re/^{188}Os$ values (61). Drill core samples (Oman) were taken over an interval of 0.8 and 1.41 m for the Khufai and Buah Formations, respectively. Sampling in core was driven by facies and TOC data, targeting organic-rich shales with up to 6% TOC. Although sampled vertically, all initial $^{187}Os/^{188}Os$ values for the Khufai and Buah Formations displayed very little internal variation (*SI Appendix*, Table S2).

Carbon and Oxygen Isotope Geochemistry. Carbonate rock samples from northwestern Canada were analyzed at both Dartmouth College and the Yale Analytical and Stable Isotope Center; 0.1- to 0.5-kg samples of limestone and dolostone were collected approximately every meter throughout detailed measured stratigraphic sections and targeted to avoid obvious fracturing or veining. The samples were then slabbed perpendicular to bedding using a lapidary saw, and ~5 to 10 mg of powder was drilled from individual laminations using a drill press with a dental carbide drill bit. Carbonate powders analyzed at Dartmouth College (JB1704, J1711, JB1707, T1701, J1713, and JB1801) were reacted with phosphoric acid (H_3PO_4) at 70 °C on a Gasbench II preparation device attached to a ThermoFinnigan DeltaPlus XL continuous flow isotope ratio mass spectrometer. $\delta^{13}C_{carb}$ and $\delta^{18}O_{carb}$ were measured simultaneously, and isotopic data are reported in standard delta notation as the per mil difference from Vienna Pee Dee Belemnite (VPDB). Precision and accuracy were monitored by running a total of 12 standards for every 76 samples using 11:3 sample/standard bracketing. The standard set includes two external standards (National Bureau of Standards [NBS]-18 and Elemental Microanalysis [EM] Carrara Marble), as well as an internal marble standard. Samples are measured relative to an internal CO_2 gas standard and then converted to the VPDB scale using the known composition of NBS-18 ($\delta^{13}C = -5.01$; $\delta^{18}O = -23.20$) and the EM-Carrara Marble ($\delta^{13}C_{carb} = 2.10$; $\delta^{18}O_{carb} = -2.01$). Measured precision was 0.1 to 0.15‰ (1σ) for $\delta^{13}C_{carb}$ and 0.15 to 0.2‰ (1σ) for $\delta^{18}O_{carb}$. Samples run at the Yale Analytical and Stable Isotopic Center (J1719) followed an identical procedure using a KIEL carbonate preparation device connected to a ThermoFinnigan MAT 253. The standard set includes the MERC ($\delta^{13}C = -48.96$; $\delta^{18}O = -16.48$), PX ($\delta^{13}C_{carb} = 2.25$; $\delta^{18}O_{carb} = -1.79$), and YM ($\delta^{13}C_{carb} = -1.59$; $\delta^{18}O_{carb} = -6.03$) standards which were calibrated against the NBS-19, NBS-18, and LSVEC international standards on the VPDB scale. Internal precision was reported as 0.1 to 0.15‰

(1σ) for $\delta^{13}C_{carb}$ and 0.1 to 0.15 ‰ (1σ) for $\delta^{18}O_{carb}$. Carbon and oxygen isotope geochemistry for Oman are from ref. 39. All data necessary for replication are included in the submission and/or publicly available from A.D.R. and M.D.C.

ACKNOWLEDGMENTS. We acknowledge Sierra Anseeuw at Yale for analytical support and Zuwena Al-Rawahi and Elena Mihaly for sampling support. We thank the Ministry of Oil and Gas of the Sultanate of Oman for permission to access samples and publish their results. The Yukon Geological Survey (YGS), ATAC Resources, and the Geological Survey of Canada provided logistical support in Yukon, Canada. M.D.C. was supported by a National Defense Science and Engineering Graduate Fellowship, K.D.B. acknowledges support from the David and Lucile Packard Foundation and Petroleum Development Oman, and T.H.B. was supported by a National Science and Engineering Research Council Doctoral Fellowship. Fieldwork in northwestern Canada was supported by the YGS, Government of Yukon Paleontology Program, Dartmouth College, the National Geographic Society (Grant CP-102R-17 awarded to E.A.S. and Grant EC-393R-18 awarded to J.F.B.), the National Science Foundation (Grant EAR-1654131 awarded to J.V.S.), and grants from the American Philosophical Society Lewis and Clark Fund (awarded to T.H.B. and J.F.B.) and Stanford McGee-Levorsen funds (awarded to T.H.B.). Thoughtful criticism from editor Paul Hoffman and two anonymous reviewers improved this manuscript.

1. D. H. Erwin *et al*., The Cambrian conundrum: Early divergence and later ecological success in the early history of animals. *Science* **334**, 1091–1097 (2011).
2. P. F. Hoffman *et al*., Snowball Earth climate dynamics and Cryogenian geology-geobiology. *Sci. Adv.* **3**, e1600983 (2017).
3. D. A. Fike, J. P. Grotzinger, L. M. Pratt, R. E. Summons, Oxidation of the Ediacaran ocean. *Nature* **444**, 744–747 (2006).
4. S. K. Sahoo *et al*., Oceanic oxygenation events in the anoxic Ediacaran ocean. *Geobiology* **14**, 457–468 (2016).
5. K. A. McFadden *et al*., Pulsed oxidation and biological evolution in the Ediacaran Doushantuo Formation. *Proc. Natl. Acad. Sci. U.S.A.* **105**, 3197–3202 (2008).
6. H. C. Halls, A. Lovette, M. Hamilton, U. Söderlund, A paleomagnetic and U–Pb geochronology study of the western end of the Grenville dyke swarm: Rapid changes in paleomagnetic field direction at ca. 585 Ma related to polarity reversals? *Precambrian Res.* **257**, 137–166 (2015).
7. R. K. Bono, J. A. Tarduno, F. Nimmo, R. D. Cottrell, Young inner core inferred from Ediacaran ultra-low geomagnetic field intensity. *Nat. Geosci.* **12**, 143–147 (2019).
8. G. P. Halverson, P. F. Hoffman, D. P. Schrag, A. C. Maloof, A. H. N. Rice, Toward a Neoproterozoic composite carbon-isotope record. *Geol. Soc. Am. Bull.* **117**, 1181–1207 (2005).
9. J. P. Grotzinger, D. A. Fike, W. W. Fischer, Enigmatic origin of the largest-known carbon isotope excursion in Earth's history. *Nat. Geosci.* **4**, 285–292 (2011).
10. S. J. Burns, A. Matter, Carbon isotopic record of the latest Proterozoic from Oman. *Eclogae Geol. Helv.* **86**, 595–607 (1993).
11. E. Le Guerroué, Duration and synchroneity of the largest negative carbon isotope excursion on Earth: The Shuram/Wonoka anomaly. *C. R. Geosci.* **342**, 204–214 (2010).
12. D. Minguez, K. P. Kodama, J. W. Hillhouse, Paleomagnetic and cyclostratigraphic constraints on the synchroneity and duration of the Shuram carbon isotope excursion, Johnnie Formation, Death Valley Region, CA. *Precambrian Res.* **266**, 395–408 (2015).
13. L. A. Derry, A burial diagenesis origin for the Ediacaran Shuram–Wonoka carbon isotope anomaly. *Earth Planet. Sci. Lett.* **294**, 152–162 (2010).
14. D. P. Schrag, J. A. Higgins, F. A. Macdonald, D. T. Johnston, Authigenic carbonate and the history of the global carbon cycle. *Science* **339**, 540–543 (2013).
15. A. M. Oehlert, P. K. Swart, Interpreting carbonate and organic carbon isotope covariance in the sedimentary record. *Nat. Commun.* **5**, 4672 (2014).
16. F. Zhang *et al*., Global marine redox changes drove the rise and fall of the Ediacara biota. *Geobiology* **17**, 594–610 (2019).
17. J. P. Pu *et al*., Dodging snowballs: Geochronology of the Gaskiers glaciation and the first appearance of the Ediacaran biota. *Geology* **44**, 955–958 (2016).
18. S. A. F. Darroch, E. F. Smith, M. Laflamme, D. H. Erwin, Ediacaran extinction and Cambrian explosion. *Trends Ecol. Evol.* **33**, 653–663 (2018).
19. A. D. Muscente, T. H. Boag, N. Bykova, J. D. Schiffbauer, Environmental disturbance, resource availability, and biologic turnover at the dawn of animal life. *Earth Sci. Rev.* **177**, 248–264 (2018).
20. S. Xiao, M. Laflamme, On the eve of animal radiation: Phylogeny, ecology and evolution of the Ediacara biota. *Trends Ecol. Evol.* **24**, 31–40 (2009).
21. S. A. Bowring *et al*., Geochronologic constraints on the chronostratigraphic framework of the Neoproterozoic Huqf Supergroup, Sultanate of Oman. *Am. J. Sci.* **307**, 1097–1145 (2007).
22. A. D. Rooney, J. V. Strauss, A. D. Brandon, F. A. Macdonald, A Cryogenian chronology: Two long-lasting synchronous Neoproterozoic glaciations. *Geology* **43**, 459–462 (2015).
23. T. H. Boag, S. A. F. Darroch, M. Laflamme, Ediacaran distributions in space and time: Testing assemblage concepts of earliest macroscopic body fossils. *Paleobiology* **42**, 574–594 (2016).
24. M. L. Droser, L. G. Tarhan, J. G. Gehling, The rise of animals in a changing environment: Global ecological innovation in the late Ediacaran. *Annu. Rev. Earth Planet. Sci.* **45**, 593–617 (2017).
25. A. G. Liu, C. G. Kenchington, E. G. Mitchell, Remarkable insights into the paleoecology of the Avalonian Ediacaran macrobiota. *Gondwana Res.* **27**, 1355–1380 (2015).
26. J. G. Gehling, M. L. Droser, How well do fossil assemblages of the Ediacara Biota tell time? *Geology* **41**, 447–450 (2013).
27. S. A. Darroch *et al*., Biotic replacement and mass extinction of the Ediacara biota. *Proc. Biol. Sci.* **282**, 20151003 (2015).
28. S. Xiao *et al*., Towards an Ediacaran time scale: Problems, protocols, and prospects. *Episodes J. Int. Geosci.* **39**, 540–555 (2016).
29. F. A. Macdonald *et al*., The stratigraphic relationship between the Shuram carbon isotope excursion, the oxygenation of Neoproterozoic oceans, and the first appearance of the Ediacara biota and bilaterian trace fossils in northwestern Canada. *Chem. Geol.* **362**, 250–272 (2013).
30. D. Condon *et al*., U-Pb ages from the Neoproterozoic Doushantuo Formation, China. *Science* **308**, 95–98 (2005).
31. S. R. Noble *et al*., U-Pb geochronology and global context of the Charnian Supergroup, UK: Constraints on the age of key Ediacaran fossil assemblages. *Geol. Soc. Am. Bull.* **127**, 250–265 (2015).
32. P. A. Allen, The Huqf Supergroup of Oman: Basin development and context for Neoproterozoic glaciation. *Earth Sci. Rev.* **84**, 139–185 (2007).
33. E. Le Guerroué, P. A. Allen, A. Cozzi, Chemostratigraphic and sedimentological framework of the largest negative carbon isotopic excursion in Earth history: The Neoproterozoic Shuram Formation (Nafun Group, Oman). *Precambrian Res.* **146**, 68–92 (2006).
34. E. L. Guerroué, P. A. Allen, A. Cozzi, Parasequence development in the Ediacaran Shuram Formation (Nafun Group, Oman): High-resolution stratigraphic test for primary origin of negative carbon isotopic ratios. *Basin Res.* **18**, 205–219 (2006).
35. A. Cozzi, J. P. Grotzinger, P. A. Allen, Evolution of a terminal Neoproterozoic carbonate ramp system (Buah Formation, Sultanate of Oman): Effects of basement paleotopography. *Geol. Soc. Am. Bull.* **116**, 1367–1384 (2004).
36. C. J. Nicholas, S. E. P. Gold, Ediacaran–Cambrian Sirab Formation of the Al Huqf region, Sultanate of Oman. *GeoArabia* **17**, 49–98 (2012).
37. K. D. Bergmann, S. A. K. A. Balushi, T. J. Mackey, J. P. Grotzinger, J. M. Eiler, A 600-million-year carbonate clumped-isotope record from the Sultanate of Oman. *J. Sediment. Res.* **88**, 960–979 (2018).
38. M. E. G. McCarron, *The Sedimentology and Chemostratigraphy of the Nafun Group, Huqf Supergroup, Oman*, (University of Oxford, 1999).
39. G. A. Forbes, H. S. M. Jansen, J. Schreurs, *Lexicon of Oman: Subsurface Stratigraphy: Reference Guide to the Stratigraphy of Oman's Hydrocarbon Basins*, (Gulf PetroLink, 2010).
40. R. Rieu *et al*., A composite stratigraphy for the Neoproterozoic Huqf supergroup of Oman: Integrating new litho-, chemo- and chronostratigraphic data of the Mirbat area, southern Oman. *J. Geol. Soc.* **164**, 997–1009 (2007).
41. I. Gomez-Perez, S. Farqani, S. Scholten, A. Rovira, B. Baloushi, "The Precambrian succession of Oman from Platform to Basin: Predicting reservoir and source rock distribution" in *European Association of Geoscientists & Engineers Seventh Arabian Plate Geology Workshop: Pre-Cambrian to Paleozoic Petroleum Systems in the Arabian Plate*, M. Al Baghli, Ed. *et al*. (EAGE, 2018), pp. 1–3.
42. D. Rabu, "Geologie de l'autochtone des montagnes d'Oman, la fênetre du Jabal Akhdar: la semelle metamorphique de la nappe ophiolitique de Samail dans les parties orientale et centrale des Montagnes d'Oman: une revue [Geology of the Oman Mountains Autochthon, Jabal Akhdar Window: metamorphic basement of the Semail ophiolitic nappe, eastern and central Oman Mountains; a review]," PhD Thesis, Pierre et Marie Curie Université, Paris VI, Paris (1987), p. 613.
43. D. Rabu, P. Nehlig, R. Jack, *Stratigraphy and Structure of the Oman Mountains*, (Bureau de Recherches Geologiques et Minieres, 1993), Vol. 221.
44. J. E. Amthor *et al*., Extinction of Cloudina and Namacalathus at the Precambrian-Cambrian boundary in Oman. *Geology* **31**, 431–434 (2003).
45. D. P. Moynihan, J. V. Strauss, L. L. Nelson, C. D. Padget, Upper Windermere Supergroup and the transition from rifting to continent-margin sedimentation, Nadaleen River area, northern Canadian Cordillera. *Geol. Soc. Am. Bull.* **131**, 1673–1701 (2019).
46. G. M. Narbonne, M. Laflamme, P. W. Trusler, R. W. Dalrymple, C. Greentree, Deep-water Ediacaran fossils from northwestern Canada: Taphonomy, ecology, and evolution. *J. Paleontol.* **88**, 207–223 (2014).
47. C. A. Carbone, G. M. Narbonne, F. A. Macdonald, T. H. Boag, New Ediacaran fossils from the uppermost Blueflower Formation, northwest Canada: Disentangling biostratigraphy and paleoecology. *J. Paleontol.* **89**, 281–291 (2015).
48. P. S. Mustard, J. A. Donaldson, R. I. Thompson, "Trace fossils and stratigraphy of the Precambrian–Cambrian boundary sequence, upper Harper group, Ogilvie Mountains, Yukon" (Current Research, Part E, Geological Survey of Canada Paper, 1988), pp. 197–203.
49. P. S. Mustard, C. F. Roots, "Rift-related volcanism, sedimentation, and tectonic setting of the Mount Harper group, Ogilvie Mountains, Yukon Territory" (Geological Survey of Canada Bulletin 492, 1997).
50. M. I. Smoliar, R. J. Walker, J. W. Morgan, Re-Os ages of group IIA, IIIA, IVA, and IVB iron meteorites. *Science* **271**, 1099–1102 (1996).
51. D. E. Canfield, A. H. Knoll, S. W. Poulton, G. M. Narbonne, G. R. Dunning, Carbon isotopes in clastic rocks and the Neoproterozoic carbon cycle. *Am. J. Sci.* **320**, 97–124 (2020).
52. J. J. Matthews *et al*., A chronostratigraphic framework for the rise of the Ediacaran macrobiota: New constraints from Mistaken Point Ecological Reserve, Newfoundland. *Geol. Soc. Am. Bull.* In press.

53. T. H. Boag, R. G. Stockey, L. E. Elder, P. M. Hull, E. A. Sperling, Oxygen, temperature and the deep-marine stenothermal cradle of Ediacaran evolution. *Proc. Biol. Sci.* **285**, 20181724 (2018).
54. B. Kendall *et al*., Uranium and molybdenum isotope evidence for an episode of widespread ocean oxygenation during the late Ediacaran Period. *Geochim. Cosmochim. Acta* **156**, 173–193 (2015).
55. S. D. Evans, C. W. Diamond, M. L. Droser, T. W. Lyons, Dynamic oxygen and coupled biological and ecological innovation during the second wave of the Ediacara Biota. *Emerg. Top. Life Sci.* **2**, 223–233 (2018).
56. E. A. Sperling *et al*., Oxygen, facies, and secular controls on the appearance of Cryogenian and Ediacaran body and trace fossils in the Mackenzie Mountains of northwestern Canada. *Geol. Soc. Am. Bull.* **128**, 558–575 (2016).
57. J. A. Higgins *et al*., Mineralogy, early marine diagenesis, and the chemistry of shallow-water carbonate sediments. *Geochim. Cosmochim. Acta* **220**, 512–534 (2018).
58. A.-S. C. Ahm, C. J. Bjerrum, C. L. Blättler, P. K. Swart, J. A. Higgins, Quantifying early marine diagenesis in shallow-water carbonate sediments. *Geochim. Cosmochim. Acta* **236**, 140–159 (2018).
59. E. C. Geyman, A. C. Maloof, A diurnal carbon engine explains ^{13}C-enriched carbonates without increasing the global production of oxygen. *Proc. Natl. Acad. Sci. U.S.A.* **116**, 24433–24439 (2019).
60. J. V. Strauss, A. D. Rooney, F. A. Macdonald, A. D. Brandon, A. H. Knoll, 740 Ma vase-shaped microfossils from Yukon, Canada: Implications for Neoproterozoic chronology and biostratigraphy. *Geology* **42**, 659–662 (2014).
61. B. Kendall, R. A. Creaser, D. Selby, ^{187}Re-^{187}Os geochronology of Precambrian organic-rich sedimentary rocks. *Geol. Soc. Lond. Spec. Publ.* **326**, 85–107 (2009).